The structural and magnetic properties of barium ferrite powders prepared by the sol–gel method*

Li Jie(李 颉)†, Zhang Huai-Wu(张怀武), Li Yuan-Xun(李元勋),
Liu Ying-Li(刘颖力), and Ma Yan-Bing(马岩冰)

School of Microelectronics and Solid-State Electronics, University of Electronic Science and Technology of China, Chengdu 610054, *China*

(Received 19 July 2011; revised manuscript received 1 September 2011)

In this paper, M-type hexagonal barium ferrite powders are synthesized using the sol–gel method. A dried precursor heated in air is analyzed in the temperature range from 50 to 1200 °C using thermo-gravimetric analysis and differential scanning calorimetry. The effects of the additives and the cacinating temperature on the magnetic properties are investigated, and the results show that single-phase barium ferrite powders can be formed. After heat-treating at 950 °C for 4h with 3 wt% additive, the coercivity and saturation magnetization are found to be 440 Oe and 57.9 emu/g, respectively.

Keywords: barium ferrite, sol–gel method, powder, magnetic property

PACS: 75.60.Ej, 75.75.Lf, 75.60.Nt **DOI:** 10.1088/1674-1056/21/1/017501

1. Introduction

Barium ferrites are a large family of ferromagnetic oxides with a hexagonal close-packed structure.[1] The first and most analyzed compound in the BaO-FeO-Fe_2O_3 ternary system is the so-called M-phase $BaFe_{12}O_{19}$, which has a magnetoplumbite structure.[2] Nowadays, barium ferrites are widely used in low-temperature co-fired ceramics (LTCC) applications because of their stable magnetic performance, high resistivity and anisotropy.[3] The electromagnetic properties of nanoferrites are very sensitive to many factors, including the method of preparation, sintering rate, sintering temperature, sintering duration and sintered additives.[4]

In this work, we report the synthesis and characterization of barium ferrite nanoparticles prepared by the sol–gel method. Detailed research has been carried out on the structural and magnetic properties of barium ferrite,[5] and it turns out that a lot of the factors, such as the addition order and the calcining temperature, can lead to different microstructures and magnetic properties of the final product. In this study, we investigate the effect of some of the technological factors on the magnetic properties of the produced barium ferrites. The structure, morphology and magnetic properties of the resultant nanocrystalline are characterized and discussed.[6−10]

2. Experiments

Using the sol–gel method, stoichiometric amounts of barium nitrate ($Ba(NO_3)_2$), iron nitrate ($Fe(NO_3)_3$) and citric acid ($C_6H_8O_7{\cdot}H_2O$) were dissolved into distilled water. The mixture was adjusted to have a pH of 7–9 by adding ammonia, and then joined in the dispersant and heated at 120 °C for 10 h to obtain a dried precursor. The Bi_2O_3, with a content ranging from 0 to 5 wt%, was added as the sintering additive to lower the temperature. Then the sample was calcined at different temperatures for 4 h at a rate of 120 °C/h to obtain a ferrite powder.

The phase, morphology and particle diameter of the samples were studied using X-ray diffraction (XRD) and a scanning electron microscope (SEM), and the magnetic properties were inspected using a vibrating sample magnetometer. Meanwhile, thermo-gravimetric analysis (TGA) and differential scanning

*Project supported by the National Basic Research Program of China (Grant No. 2007CB310407), the Science Fund for Creative Research Groups of the National Natural Science Foundation of China (Grant No. 61021061), the National Natural Youth Fund of China (Grant No. 61001025), and National Programs for Science and Technology Development of Guangdong Province, China (Grant No. 2010B090400314).

†Corresponding author. E-mail: lijie8594@gmail.com

© 2012 Chinese Physical Society and IOP Publishing Ltd

calorimetry (DSC) were carried out on a Mettler Toledo TGA/DSC thermal analyzer at a heating rate of 10 °C/min in air.

3. Results and discussion

Figure 1 shows the TGA and DSC results obtained with the samples heated in air from 50 to 1200 °C. It describes the evolution of the precursor of the $BaFe_{12}O_{19}$ sample (before sintering) as a function of temperature up to 1200 °C. This technique allows us to observe the weight variation of the sample with rising temperature (TGA curve), as well as its rate of change (DSC curve). The TGA curve exhibits a three-stage mass loss happening at 100–120 °C, 700–850 °C, and 1100–1150 °C, respectively. The loss in the first step is caused by the evaporation of the physically adsorbed water in the gel. The combustion of the carbon-based content occurs at 800 °C, which leads to the second step loss, and the weight loss of the sample is about 2.7 wt%. The third step is the formation of the spinel phase, which starts at 1100 °C, and the final step is thought to be caused by the growth of the crystal phase. Meanwhile, the DSC curve of the as-prepared barium ferrite sample is also shown in Fig. 1. The curve shows an exothermic peak centred around 800–1100 °C, which corresponds to the phase transition from amorphous to crystalline. The broad exotherm could be explained by the wide size distribution of the particles. Based on these results, a heating region for the coating process is determined to be at temperatures between 800 and 1100 °C without any additives.

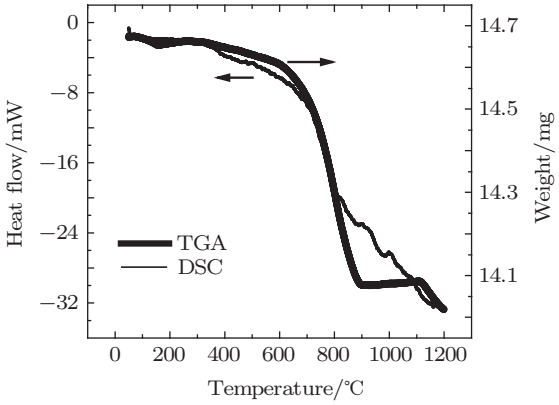


Fig. 1. The DSC and TGA curves of the dried precursor.

In order to find the exact temperature for the formation of the M-type barium ferrite, the precursor powders were heat-treated at 850, 900 and 950 °C, and the corresponding XRD patterns of the $BaFe_{12}O_{19}$ samples are shown in Fig. 2, which gives the results of such an investigation for the $BaFe_{12}O_{19}$ powders. It can be found that the products obtained with the Bi_2O_3 additive at 900 and 950 °C are pure phase hexagonal $BaFe_{12}O_{19}$, which does not exist in the sample sintered at 850 °C. For the sample sintered at 850 °C, the α-Fe_2O_3 phase is clearly seen. However, when the temperature goes up to 900 and 950 °C, the α-Fe_2O_3 phase disappears, and the single phase of barium ferrite appears. One of the reasons leading to the above result is the additive, which promotes the liquid phase sintering process by introducing Bi_2O_3 accompanied by the substance transmission process. Another reason may be that the sol–gel method can realize molecular level mixing and that the dispersant can improve the activity of the reactants, which helps to form the single-phase spinel barium ferrite.

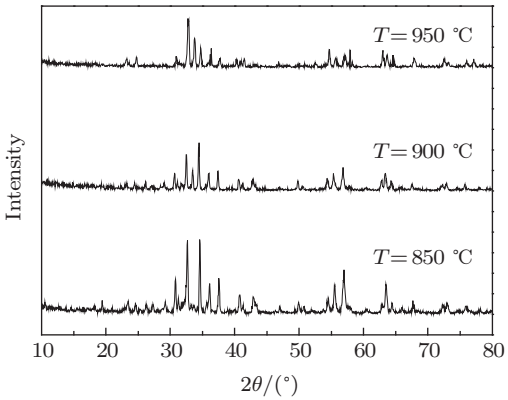


Fig. 2. The XRD for $BaFe_{12}O_{19}$ powders heat-treated at different temperatures.

As we know, the high magnetic properties of ferrite are mostly dependent on the microstructures of the pre-sintered products. In order to show the difference between the samples sintered at different temperatures, SEM images of the samples are presented in Fig. 3. From the two SEM images, it can be seen that the grains inside the samples begin to grow bigger and more uniform as the sintering temperature increases from 900 to 950 °C. The pre-sintered product at the pre-sintering temperature of 900 °C is shown in Fig. 3(a). It is obvious that the size range of the crystal grains is from 0.5 to 2 μm, and the distribution of the particles is uneven. In contrast, as shown in Fig. 3(b), the grain sizes of the samples pre-sintered at 950 °C are mostly 1 μm and uniform, so it is surprising that the magnetic property of the latter is higher than that of the powder sintered at 900 °C. It can be seen that it is important to control the sizes of the grains

in the pre-sintered samples to obtain a high-property ferrite powder.

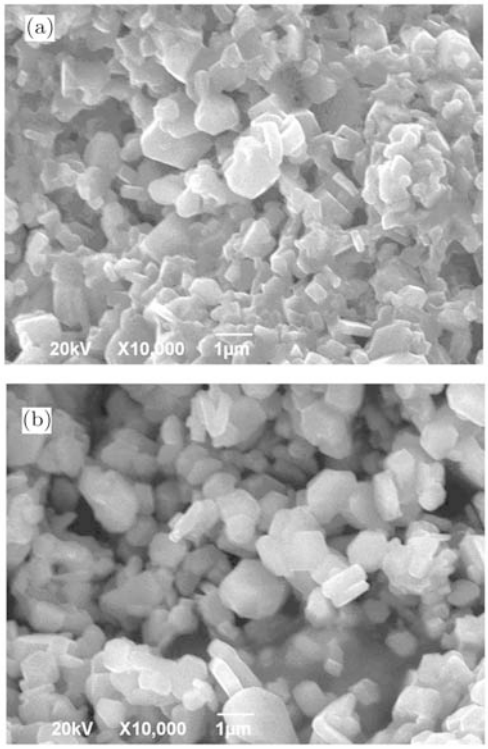


Fig. 3. SEM images of samples sintered at (a) 900 and (b) 950 °C.

The magnetic hysteresis loops for the as-prepared sample were obtained using a vibrating sample magnetometer. Figure 4 shows the hysteresis loop of the barium ferrite nanoparticles obtained at the calcination temperature of 950 °C. The saturation magnetization of the sample reaches 57.9 emu/g. The variations in saturation magnetization, M_s, and the coercivity, H_c, of these samples with temperature and additive content are presented in Fig. 5. It can be found that with the increase in the amount of additive, M_s and H_c both experience fluctuation, which can be described as follows. The M_s increases at first, and then reaches a peak value when the additive amount is 3 wt%. Then it dramatically decreases with the increase in the amount of additive, when the amount of Bi_2O_3 exceeds 3 wt%. The fact that is responsible for these results is that the liquid-phase sintering process lowering the sintering activation energy helps improve the high densifications to some degree, and the addition of non-magnetic Bi_2O_3 decreases the value of M_s. At the same time, H_c increases first, and then reaches a minimum value when the amount of Bi_2O_3 reaches 3 wt%. This phenomenon leads to the growth of crystalline grains under the effectiveness of a specific amount of Bi_2O_3.

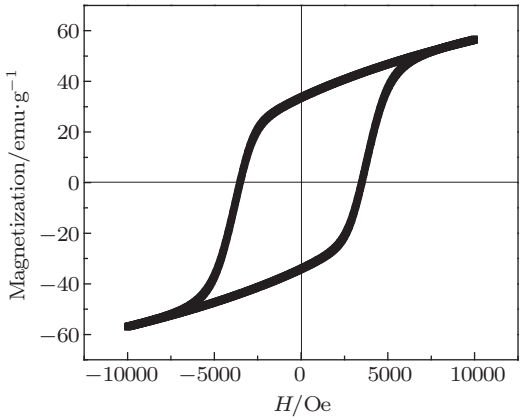


Fig. 4. The magnetic hysteresis loop of the powder $BaFe_{12}O_{19}$ sample sintered at 950 °C.

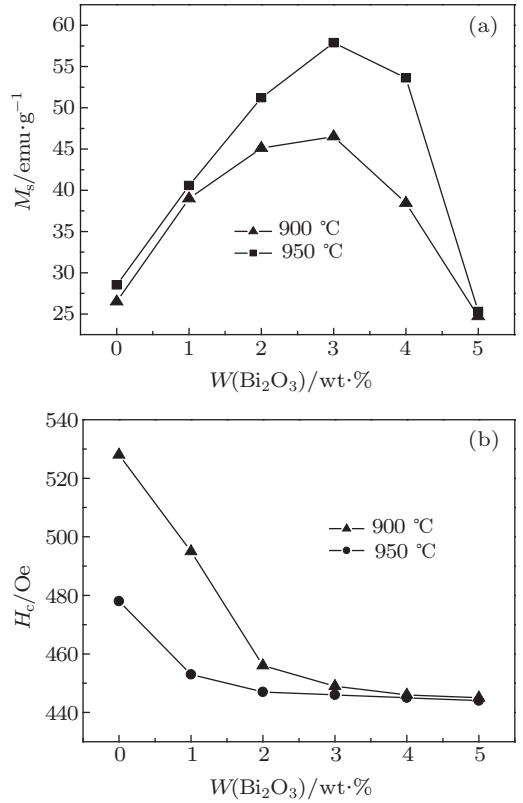


Fig. 5. (a) Saturation magnetization and (b) coercivity of samples obtained at different sintering temperatures versus the content of the additive.

4. Conclusion

Barium ferrite nanoparticles with a hexagonal phase were successfully synthesized by using the sol–gel method, and were then calcined at 850–950 °C with a Bi_2O_3 additive. The results show that single-phase barium ferrite powders can be formed after heat-treating at 950 °C for 4 h with a 3 wt% additive. Coercivity, H_c, and saturation magnetization, M_s, are 440 Oe and 57.9 emu/g, respectively, so there

should be potential applications in LTCC technology for the fabrication of electronic devices.

References

[1] Su H, Zhang H W, Tang X L and Liu B Y 2009 *J. Phys.* **152** 012064

[2] Gao L Q, Yu G J, Wang Y and Wei F L 2011 *Chin. Phys.* B **20** 027503

[3] Liu Y L, Li Y X, Zhang H W, Chen D M and Wen Q Y 2010 *J. Appl. Phys.* **107** 09A507

[4] Xiang J, Shen X Q, Song F Z and Liu M Q 2009 *Chin. Phys.* B **18** 4960

[5] Dolia S N 2010 *J. Phys.* **200** 072026

[6] Jadhav S P, Toksha B G, Jadhav K M and Shinde N D 2010 *Chin. J. Chem. Phys.* **23** 459

[7] Xu F, Bai Y, Ai F and Qiao L J 2008 *Chin. Phys.* B **17** 4052

[8] Ramay S M , Siddiqi S A, Atiq S, Awan M S and Riaz S 2010 *Chin. J. Chem. Phys.* **23** 591

[9] Li Q L, Chang C B, Zhang W and Zhang H 2010 *Chin. J. Chem. Phys.* **23** 680

[10] Thakur S, Katyal S C, Gupta A, Reddy V R and Singh M 2010 *J. Phys.* **217** 012101